in which the metal is coordinated to the carbene lone pair of CO_2^{2-}. This optimization leads to a rearrangement toward the C_{2v} structure.

IV. Cyclic $CaCO_2$. Final refinements of the preliminary results of section II are performed with the 3-21+G basis on all non-metal atoms (Table III). Both the C_s and C_{2v} optimizations converge to stable geometries. In the former structure, the O-C-O angle remains about the same as in the isolated anion calculation, but there is a considerable difference between the CO bond lengths. In the C_{2v} isomer, the O-C-O angle is narrower and the CO distances are longer. These results, plus those for the Mg-containing C_{2v} isomer, indicate that the anionic fragment has considerable flexibility in binding to the metal ions. Further perturbations are applied to these structures to see if breaking symmetry, e.g., destroying planarity, leads to lower energy. None of these perturbations has any effect on the final optimized structures. Total energy calculations on the two isomers are improved by adding second-order correlation corrections. A final improvement adds d functions[15b] to O and C atoms as well as correlation. The correlated calculations yield energies that are quite close.

Conclusions

The present study shows that the interaction of MgO with CO results in stable linear and C_{2v} four-membered ring structures.[21] The binding energy associated with the cyclic structure is much larger than those of the linear systems. The interaction of CaO with CO yields stable C_s three-membered ring and C_{2v} four-membered ring $CaCO_2$ complexes with nearly equivalent binding energy values. The cyclic structures resemble coordination of a CO_2^{2-} anion with an M^{2+} cation, and the anion has considerable flexibility in binding.

Acknowledgment. Dr. P. J. Hay of Los Alamos National Laboratory provided information on d basis functions and contraction schemes for Ca, for which we are most grateful. This work was supported by an Army Research Office grant to K.J.K.

Registry No. CO, 630-08-0; MgO, 1309-48-4; CaO, 1305-78-8.

(21) For similar structures resulting from metal interactions with CO_2, see: Mascetti, J.; Tranquille, M. *J. Phys. Chem.* **1988**, *92*, 2177.

Photoactivation of H_2O by *p*-Benzoquinone and the Role of Mn^{III} Complexes in O_2 Evolution: Molecular Orbital Theory

Mohamed K. Awad and Alfred B. Anderson*

Contribution from the Chemistry Department, Case Western Reserve University, Cleveland, Ohio 44106. *Received April 25, 1988*

Abstract: A mechanistic quantum chemical study is made of the photogeneration of O_2 from H_2O coordinated to active Mn^{III} complexes in the presence of *p*-benzoquinone, as studied experimentally by Ashmawy and co-workers. The abstraction of H from H_2O by $\pi^* \leftarrow n$ optically excited *p*-benzoquinone is explained, using molecular orbital theory, as being caused by the H accepting ability of the O' in the excited quinone. In the absence of active Mn complexes, hydroquinone and 2-hydroxy-*p*-benzoquinone are the photoproducts. In the presence of active complexes, and in acidic solution to prevent these reactions, H_2O coordinated to Mn^{III} is photoactivated, leading to hydroquinone and OH strongly bound to Mn^{IV}. Following deprotonation, stable di-μ-oxo Mn^{IV} dimers form which disproportionate via a 4Mn complex (reminiscent of proposed photosystem II processes by plants) to O_2 and a stable O-bridged Mn^{III} dimer. According to the calculations, this last step is rate limiting. It is shown that dimerization of the Mn complexes is the key to O_2 generation in the active systems, and this is controlled by the ligand structure.

In plant photosynthesis, dioxygen is evolved from the catalyzed photodecomposition of water. The generation of one molecule of oxygen from two molecules of water requires the transfer of four electrons:

$$2H_2O \xrightarrow{h\nu} O_2 + 4H^+ + 4e^- \quad (1)$$

It is generally believed that four atoms of Mn in the reaction center are essential for oxygen evolution in biological photosystem II (PSII) activity.[1] At least two of these Mn atoms occur in a binuclear species with a Mn-Mn separation of ca. 2.7 Å.[2]

Kambara et al.[3] devised a model for photosynthetic water oxidation to provide a possible mechanistic explanation. In this model the four Mn^{III} cations are divided into two groups, [Mn] complexes in a hydrophobic cavity and (Mn) complexes on a hydrophilic surface. Following oxidation to Mn^{IV}, caused by electron transfer to light-absorbing centers, each of the two hydrophobic Mn complexes oxidizes a coordinated H_2O and the protons transfer to the hydrophilic Mn complexes along the hydrogen bonds between their respective ligand H_2O molecules. It is proposed that the O_2 molecule in a complex of the form Mn^{III}-O_2-Mn^{III} is replaced by two H_2O molecules, which completes the cycle.

An alternative mechanism has been given by Brudvig and Crabtree[4] for photosynthetic oxygen evolution based on a structural conversion of an Mn_4O_6 complex to an Mn_4O_4 complex. They proposed that Mn_4O_4 undergoes a series of photoactivated oxidation steps and structural rearrangements to the Mn_4O_6 form which has two O^{2-} or OH^- coordinated in it. The formation of an O-O bond and the loss of O_2 and the recreation of the starting Mn_4O_4 cluster completes the cycle.

Several other models have been devised in attempts to explain the role of manganese and the mechanism of oxygen evolution in the photosynthetic process.[5-7] However, the true mechanism or mechanisms for oxygen evolution remain unproved.

Recently there has been an interest in the photogeneration of O_2 from H_2O using soluble Mn^{III} complexes.[8a] The photolysis

(1) Dismukes, G. C. *Photochem. Photobiol.* **1986**, *43*, 99.
(2) Yachandra, V. K.; Guiles, R. D.; McDermott, A.; Britt, R. D.; Dexheimer, S. L.; Sauer, K.; Klein, M. P. *Biochim. Biophys. Acta.* **1986**, *850*, 324.
(3) (a) Kambara, T.; Govindjee, *Proc. Natl. Acad. Sci. U.S.A.* **1985**, *82*, 6119. (b) Govindjee,; Kambara, T.; Coleman, W. *Photochem. Photobiol.* **1985**, *42*, 187.
(4) Brudvig, G. W.; Crabtree, R. H. *Proc. Natl. Acad. Sci. U.S.A.* **1986**, *83*, 586.
(5) Amesz, J. *Biochim. Biophys. Acta* **1983**, *726*, 1.
(6) Goodin, D. B.; Yachandra, V. K.; Britt, R. D.; Sauer, K.; Klein, M. P. *Ibid.* **1984**, *767*, 209.
(7) Sauer, K. *Acc. Chem. Res.* **1980**, *13*, 249.

0002-7863/89/1511-0802$01.50/0 © 1989 American Chemical Society

Table I. Atomic Parameters Used in the Calculations; Principal Quantum Numbers, IP (eV), Orbital Exponents, ζ (au), and Respective Linear Coefficients, c, for Double-ζ d Orbitals

	s			p			d					
atom	n	IP	ζ	n	IP	ζ	n	IP	ζ_1	c_1	ζ_1	c_2
N	2	20.33	1.9237	2	14.53	1.917						
O	2	28.48	2.246	2	13.62	2.227						
H	1	13.6	1.2									
Mn^{III}	4	10.13[a]	1.65[a]	4	7.85[a]	1.35[a]	3	11.7[a]	5.15	0.5470	2.1	0.6050

[a] See ref 13.

mechanism, which is clearly different from that of plant photosynthesis, is the topic of the present theoretical investigation. One step of this O_2-generating mechanism will be postulated to involve an Mn_4 intermediate and in this way bears some similarity to the process proposed by Brudvig and Crabtree.

Over 50 manganese(III) Schiff-base complexes having the stoichiometry $[LMn^{III}H_2O]ClO_4$ [L = *N,N'*-R-bis(salicylaldimine)] were prepared by Ashmawy et al.[8a] Three of them, with R = $(CH_2)_2$, $(CH_2)_3$, and $(CH_2)_4$, were found to have significant photoactivity, liberating dioxygen and reducing *p*-benzoquinone to hydroquinone when irradiated with visible light. Structure determinations and conductivity measurements showed that, for the three active complexes, there was a monomer–dimer equilibrium in aqueous solution:

$$2[LMn^{III}H_2O]^+ \rightleftarrows [\{LMn^{III}H_2O\}_2]^{2+} \quad (2)$$

All the active complexes exhibited a band at 590 nm in the electronic absorption spectrum that was absent for the inactive complexes. It was shown by IR analysis that the water which was photolyzed was coordinated to the Mn^{III}. It was argued that the photoreduction of *p*-benzoquinone probably proceeded by an H atom transfer mechanism rather than stepwise protonation and reduction,[8b] but the details of the transfer were not established. The Mn complex was converted to $[\{LMn^{III}\}_2O]$ as a black precipitate during irradiation, so the process was not catalytic.

Ononye et al.[9a,b] and Bridge and Porter[9c] studied the photochemistry of benzoquinone at pH 7 and greater in aqueous solutions and suggested that excited-state quinone abstracts a hydrogen atom directly from water. Ononye et al. observed the formation of hydroxyl radicals by chemical trapping. The final products were hydroquinone and 2-hydroxybenzoquinone. Ashmawy, restricting the pH to values <7 to prevent reactions with uncoordinated water, found no dioxygen evolution when *p*-benzoquinone or the Mn^{III} complexes were separately irradiated.[8a]

In the present molecular orbital study the atom superposition and electron delocalization molecular orbital (ASED-MO) theory is used to explain the photoactivation of H_2O by *p*-benzoquinone and to test possible mechanistic steps for oxygen evolution during water photolysis by the aqueous manganese complexes in the presence of *p*-benzoquinone.

Theoretical Method. The electronic charge density function of a molecule can be partitioned into components. The atom superposition and electron delocalization molecular orbital (ASED-MO) method is a semiempirical theory based on partitioning molecular density function (ρ_{mol}) into rigid atomic components and a nonrigid or nonperfectly following (ρ_{npf}) component.[10] For the example of a diatomic molecule ab,

$$\rho_{mol} = \rho_a + \rho_b + \rho_{npf} \quad (3)$$

where ρ_a and ρ_b are atomic charge densities centered on nucleus a and nucleus b, and ρ_{npf} is an electron delocalization or bond charge density. According to the electrostatic theorem, the force on nucleus a has two nonzero components, a repulsive one due to the nucleus and electronic charge distribution of atom b and an attractive force due to ρ_{npf}. These forces are integrated, yielding the potential energy $E(R)$, where R is the internuclear distance:

$$E(R) = E_r(R) + E_{npf}(R) \quad (4)$$

$E_r(R)$ is the repulsive energy due to atom superposition and $E_{npf}(R)$ is the attractive energy due to electron delocalization. E_{npf} is approximated as the change in the total one-electron valence orbital energy that is due to bond formation:

$$E \simeq E_r + \Delta E_{MO} \quad (5)$$

ΔE_{MO} is found by using a modified extended Hückel Hamiltonian.[10] When this approximation to E_{npf} is employed, the more electronegative atom is used to provide the density function for E_r. The ASED-MO theory has been applied in numerous diverse studies of molecular structures, reaction mechanism, and electronic and vibrational properties. The input data consist of valence-state Slater orbital exponents[11] and ionization potentials[12] (VSIP) for the constituent atoms. These parameters are sometimes altered, particularly in treating ionic heteronuclear molecules, to ensure reasonably accurate calculations of ionicities and bond lengths in diatomic fragment molecules. In this way electronic charge self-consistency is taken into account.[13] The diatomic parameters are used in studying larger molecules. In the present work, unshifted atomic parameters for C, N, O, and H atoms given in Table I are used. The Mn parameters, also in Table I, are approximated for the 3+ oxidation state. Shifts in Mn ionization potential parameters of ±1 eV and in 3d exponents of ±0.2 from the tabulated values produced only small changes in structures and relative stabilities for the complexes; the present set yielded reasonable charge transfer to the ligands.

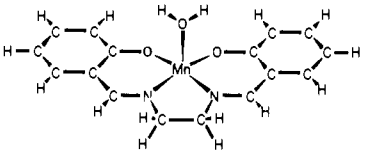

Figure 1. Structure of the $[LMn^{III}H_2O]^+$ complex. Standard bond lengths and angles except for the Mn–OH_2 distance, which is calculated to 2.17 Å.

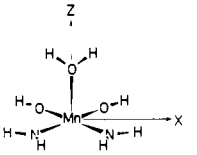

Figure 2. $[LMn^{III}H_2O]^+$ structure using truncated ligand models. The Mn–OH_2 distance is 2.05 Å.

Structural Models for Mn^{III} Monomer and Dimer. The $[LMn^{III}H_2O]^+$ complex structure is shown in Figure 1. Standard bond lengths (C=C 1.40 Å, C—C 1.54 Å, C=N 1.32 Å, C—N 1.48 Å, C—O 1.36 Å, CH 1.09 Å) and 120° bond angles are used

(8) (a) Ashmawy, F. M.; McAuliffe, C. A.; Parish, R. V.; Tames, J. *J. Chem. Soc., Dalton Trans.* **1985**, 1391. (b) Tames, J. Ph.D. Thesis, University of Manchester, 1981.
(9) (a) Ononye, A. I.; McIntosh, A. R.; Bolton, J. R. *J. Phys. Chem.* **1986**, *90*, 6266. (b) Ononye, A. I.; Bolton, J. R. *J. Phys. Chem.* **1986**, *90*, 6270. (c) Bridge, N. K.; Porter, G. *Proc. R. Soc. London, A* **1958**, *244*, 259, 276.
(10) Anderson, A. B. *J. Chem. Phys.* **1975**, *62*, 1187.
(11) (a) Richardson, J. W.; Niewpoort, W. C.; Powell, R. R.; Edgell, W. F. *J. Chem. Phys.* **1962**, *36*, 1057. (b) Clementi, E.; Raimondi, D. L. *J. Chem. Phys.* **1963**, *38*, 2686. (c) Basch, H.; Gray, H. B. *Theor. Chim. Acta* **1966**, *4*, 367.
(12) (a) Lotz, W. *J. Opt. Soc. Am.* **1970**, *60*, 206. (b) Moore, C. E. Atomic Energy Levels. NBS Circ. 467, National Bureau of Standards, U.S. Government Printing Office: Washington, DC, 1958.
(13) Anderson, A. B.; Grimes, R. W.; Hong, S. Y. *J. Phys. Chem.* **1987**, *91*, 4245.

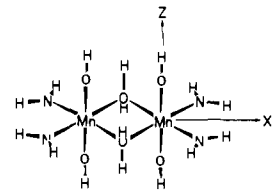

Figure 3. H_2O-bridged Mn^{III} dimer structure using truncated ligands and assuming octahedral ligand (excluding H_2O) coordination; Mn–OH_2 and Mn–Mn distances are 2.16 and 2.80 Å, respectively.

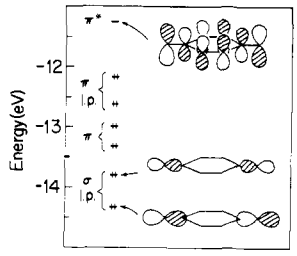

Figure 4. Calculated electronic structure of *p*-benzoquinone.

in the calculations. The central metal atom is high-spin $3d^4$ Mn^{III} with approximately square-planar coordination to the dianion O_2N_2 tetradentate Schiff base, L, and with the H_2O molecule perpendicular to the plane to form a pyramid. The N and RO^- coordinate to Mn^{III} by lone-pair donation. The Mn–O bonds also have an ionic component. Associated with the complex is a perchlorate (1–) anion. The Mn^{III} position is predicted by ASED-MO calculations. The strength of the Mn–O bonds accounts for their predicted shortness (1.61 Å) when compared to the Mn–N bonds (2.01 Å). In aqueous solutions this monomer is thought to be in equilibrium with a dimer with bridging H_2O ligands. The ligands in the dimer are highly distorted with Mn^{III} in a pseudooctahedral environment. For simplicity, two NH_2^- and two OH groups are used to model each quadridentate ligand in the monomer and dimer structures (Figures 2 and 3), assuming octahedral angles and the same Mn–ligand bond lengths as above and 1.04 Å for NH and 1.03 Å for OH.

Photochemistry of *p*-Benzoquinone in Aqueous Solutions. Ashmawy[8a] and co-workers showed the importance of having *p*-benzoquinone present as the hydrogen acceptor during water photolysis in the presence of the Mn^{III} complexes. They suggested that the conversion of quinone to hydroquinone was not achieved by proton transfer followed by electron transfer, but directly from H atom addition.[8a,b] The primary step was proposed to be hydrogen abstraction from H_2O by excited *p*-benzoquinone, which should lead to a highly reactive free hydroxyl radical:[9a,b]

$$H_2O + p\text{-}O_2C_6H_4 \xrightarrow{h\nu} OH^\bullet + p\text{-}O_2C_6H_5^\bullet \quad (6)$$

The overall reaction is

$$3p\text{-}O_2C_6H_4 + 2H_2O \xrightarrow{h\nu} p\text{-}(OH)_2C_6H_4 + 2p\text{-}O_2C_6H_3OH \quad (7)$$

Light absorption at 425 nm in aqueous solution causing a $\pi^* \leftarrow n$ transition is responsible for the reaction. Hashimoto et al.[14] could not detect hydrogen peroxide, which indicates the OH radicals do not couple under the experimental conditions employed.

ASED-MO calculations were used first to investigate the mechanism of reduction of *p*-benzoquinone to the semiquinone radical during water photolysis in the absence of the Mn^{III} complex. The calculated *p*-benzoquinone electronic structure, assuming 120° bond angles and standard bond lengths, is in Figure 4. For *p*-benzoquinone in the ground state, an endothermic reaction, uphill by 1.6 eV, was found for the first H abstraction. From standard enthalpies it can be deduced that hydrogenation of *p*-benzoquinone according to the reaction

$$H_2O + BQ \rightarrow BQH_2 + O \quad (8)$$

(14) Hashimoto, S.; Kano, K.; Okamoto, H. *Bull. Chem. Soc. Jpn.* **1972**, *45*, 966.

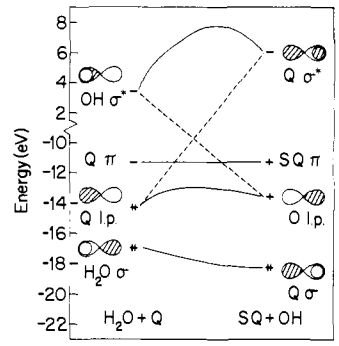

Figure 5. Orbital correlation during H transfer between OH and *p*-benzoquinone.

is uphill by 3.7 eV. The calculations produce an energy of 2.8 eV. A stability gain of 1.5 eV occurred for H abstraction when *p*-benzoquinone had an electron promoted from an oxygen lone-pair orbital to a ring π^* orbital. The calculated excitation energy is 3.06 eV, close to the 2.92 eV measured value. This is from the lower of the two lone-pair orbitals shown in Figure 4, which has a larger amplitude on the oxygen atoms. The hole site has the ability to abstract a hydrogen atom from water to form a semiquinone without the energetic expense of promoting an electron to the ring π^* orbital, as must occur for ground-state *p*-benzoquinone. This can be understood from the correlation diagram in Figure 5. The OH σ orbital energy is slightly stabilized when the hydrogen moves to the oxygen of *p*-benzoquinone. The π orbital energies remain unaffected by this reaction due to the model structure used, but the lengthening of the CO bond due to hydrogenation would cause a slight stabilization of the π orbital in Figure 5. An avoided crossing is shown; the upper curve deflects up because of the short O–O distance along the reaction path, which makes the H 1s orbital antibonding to both O 2p orbitals. A test calculation showed that when the oxygens are far enough apart the upper curve bends down, giving it the appearance of a textbook avoided crossing. The ability of chemically generated and photogenerated O^- to abstract H from CH_4 is well-known, and the explanation is similar.[15]

These results suggest that, during the photolysis of coordinated water in the manganese complex, the excited *p*-benzoquinone can be reduced by abstracting the first hydrogen atom from coordinated water to form a semiquinone radical. In the absence of the Mn complex it is necessary to go to higher pH to form hydroquinone because at higher pH the reaction

$$BQ^* + H_2O \rightarrow BQ^{\bullet-} + OH^\bullet + H^+ \quad (9)$$

is more exothermic.[9b] The hydroquinone product BQH_2 forms rapidly from the semiquinone radical anion:[9b,16]

$$2H^+ + 2BQ^{\bullet-} \rightarrow BQ + BQH_2 \quad (10)$$

The strength of the Mn–OH bond makes eq 9 highly exothermic and is also responsible for the absence of 2-hydroxybenzoquinone as a photoproduct in the Mn^{III} solution. The proposed mechanism in H_2O has OH binding to BQ to give a reactive BQ–OH$^\bullet$ intermediate that hydrogenates BQ:[9a,b]

$$OH^\bullet + BQ \rightarrow BQOH^\bullet \quad (11)$$

$$BQOH^\bullet + BQ \rightarrow HO\text{-}BQ + BQH^\bullet \quad (12)$$

It is clear that when OH$^\bullet$ is strongly bound in the Mn complex, 2-hydroxybenzoquinone formation by reactions 11 and 12 is impossible.

No mechanism other than that shown in reactions 9 and 10 has been proposed for hydroquinone formation. It seems that in the presence of the Mn^{III} complex, when this reaction was run at low pH in order to avoid these reactions, hydroquinone is most

(15) Anderson, A. B.; Ray, N. K. *J. Am. Chem. Soc.* **1985**, *107*, 253. Ward, M. D.; Brazdil, J. F.; Mehandru, S. P.; Anderson, A. B. *J. Phys. Chem.* **1987**, *91*, 6515.

(16) Adams, G. E.; Michael, B. D. *Trans. Faraday Soc.* **1967**, *63*, 1171.

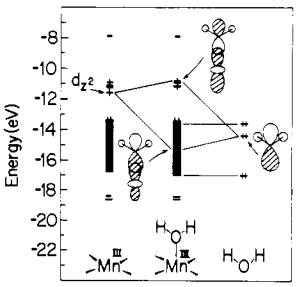

Figure 6. Bonding interactions between H_2O and Mn^{III} in the $[LMn^{III}H_2O]^+$ complex.

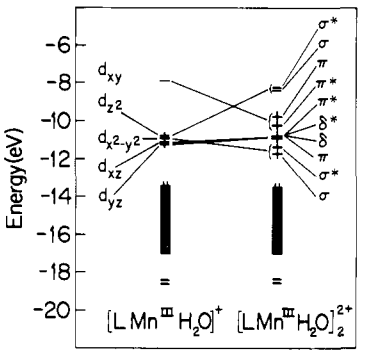

Figure 7. Correlation diagrams for two $[LMn^{III}H_2O]^+$ monomers and the $(H_2O)_2$-bridged dimer of Figures 2 and 3.

likely to form by a second hydrogenation of semiquinone. The hydrogen source will again be a coordinated H_2O.

Proposed Mechanism for O_2 Formation by the Mn^{III} Complexes. The principal stages of the photosystem II process are believed to be light trapping by P680, with electron promotion to the reducing side of photosystem II, the oxidizing side then oxidizes Mn^{III} by means of electron transfer through a connecting species Z, and H_2O oxidation commences at the Mn^{IV} center.[3] In the present work, light absorption by *p*-benzoquinone appears to account for the photoactivity.

ASED-MO calculations were performed by using the model ligand structures (Figures 2 and 3) to suggest the mechanism of photodecomposition of water coordinated to the Mn^{III} complex. The resulting mechanism leads to the formation of O_2, $2H^+$, hydroquinone, and the Mn^{III}–O–Mn^{III} complex observed by Ashmawy et al.[8a]

Calculations yield 0.7 eV for the binding energy of H_2O in the Mn^{III} monomer (Figure 2). The optimized Mn^{III}–OH_2 bond length is 2.05 Å, which is somewhat shorter than that found for the full complex. The weak bonding is characteristic of H_2O lone-pair σ-donation bonding as shown in Figure 6. The H_2O-bridged Mn^{III} dimer (Figure 3) is calculated to be less stable than two H_2O-coordinated monomers by 0.5 eV. The orbital correlation diagram is in Figure 7. This is qualitatively consistent with the experimental evidence,[8a] which suggests that there is an equilibrium between the monomer and dimer. In the following, we study dehydrogenation of H_2O coordinated in the monomer as the first step, followed by a dimerization step. The energetics would be essentially the same if dehydrogenation of H_2O-bridging ligands in the dimer is actually the first step. There is a good chance, as discussed below, that the dimer is the initial reactant.

For the hydrogen atom abstraction from coordinated H_2O by photoactivated quinone, a stability gain of 5.6 eV is calculated. This is greater than 1.6 eV found above for the free H_2O molecule because a strong Mn^{IV}–OH^- bond is formed. Deprotonation as the first step might be expected because H_2O coordinated to Mn^{III} is a weak acid,[17] but the pH of this particular reacting system is neutral.[8b] As expected, OH• binds strongly, with a MnO distance of 1.64 Å and energy of 3.8 eV, because of the charge transfer shown in Figure 8. Either a di-μ-hydroxo or di-σ-bridged di-

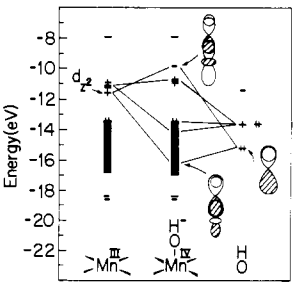

Figure 8. Bonding interactions between OH and Mn^{III} in the $[LMn^{IV}OH]^+$ complex.

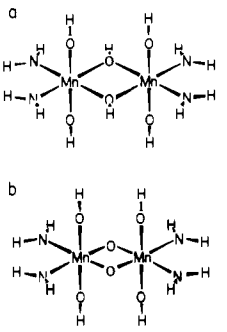

Figure 9. Calculated structures of the di-μ-hydroxo and di-μ-oxo Mn^{IV} dimer complexes.

hydroxo Mn^{IV} dimer might be expected to form if deprotonation of the OH ligand is slow. The calculations yield 1.66 eV for dimerization to the di-μ-hydroxo structure (Figure 9) and indicate that the di-σ bridged species is unstable. The Mn^{IV}–OH bond length is 1.77 Å, and though the Mn–Mn distance is 2.7 Å, the Mulliken overlap population is negative, indicating the absence of a Mn–Mn bond. Deprotonation of the di-μ-hydroxo complex yields a di-μ-oxo Mn^{IV} complex (Figure 9) with Mn^{IV}–Mn^{IV} and Mn^{IV}–O bond lengths of 2.62 and 1.71 Å, respectively. These compare well with an EXAFS study of the photosystem II which yielded respective Mn–Mn and Mn–O distances of 2.7[2] and ~1.7 Å.[18] If, on the other hand, the $[LMn^{IV}OH]$ monomers deprotonate first, then dimerization of $[LMn^{IV}O)$ will yield the di-μ-oxo Mn^{IV} complex.

The di-μ-oxo Mn^{IV} complex is calculated to be stable with respect to reductive elimination of O_2 by 8.66 eV when H_2O ligands coordinate to the Mn^{II} monomers that are formed. This is too high an energy to occur and, moreover, Mn^{II} is never observed by ESR in the experiment.[8] The overall reduction, however, requires the formation of $^1/_2O_2$ and the $[LMn^{III}OMn^{III}L]$ precipitate. This means the μ-oxo dimer would have to disproportionate, which would require two dimers to come together and go through a 4Mn intermediate, reminding one of proposed mechanisms for photosystem II. The calculated energy for forming O_2 and two dimer precipitate molecules is uphill by 5.80 eV. This would reduce to 3.45 eV when a correction is made for the theoretically underestimated O_2 bond strength of 2.97 eV. The effects of oxidation-state changes are inadequately approximated in ASED-MO calculations, so it is probable that the binding of O_2 in the di-μ-oxo Mn^{IV} complex is too strong; a small reduction could yield 0.83 eV for the elimination process, which is the overall activation energy for O_2 evolution.[8a]

The overall reaction

$$2H_2O + BQ + 2[LMn^{III}H_2O]^+ \rightarrow \frac{1}{2}O_2 + H_2BQ + 2H_3O^+ + [LMn^{III}]_2O \quad (13)$$

is calculated to be exothermic by 1.47 eV. The overall energetics should be reasonably accurate because there is no change in the Mn oxidation state. The ~1.2 eV underestimate of the $^1/_2O_2$ bond strength is largely cancelled by the 1-eV underestimate of

(17) Wells, C. F. *Nature (London)* **1965**, *205*, 693.

(18) Calvin, M. *Science* **1974**, *184*, 375.

the H_2BQ formation energy. The stability of the Mn–O bonds in the product is an important contributing factor to the calculated exothermicity. For the electronic structure of this complex a Mn 3d occupation of three unpaired electrons for Mn is assumed, which is suggested by the observation[8] of a 3.3 μ_B magnetic moment.

Discussion and Conclusions

It was noted earlier that the photoactive Mn^{III} complexes all absorb at 590 nm and the inactive ones do not. Furthermore, the complex with highest activity, R = $(CH_2)_3$, showed the strongest 590-nm band. It is probable that this absorption is characteristic of dimerization. Electronic structures for our simplified H_2O-coordinated monomer and H_2O-bridged dimer are shown in Figure 7. It may be seen that the monomer Mn 3d set of orbitals is broadened by dimerization. The lowest ligand to Mn^{III} charge-transfer excitation is 0.6 eV less in energy in the dimer. Considering the approximations of our structural model for the dimer and the theoretical method, this corresponds well with the 0.8 eV difference between the first dimer peak and the first peak for the R = o-C_6H_4 monomer complex (~425 nm).[8a] Furthermore, manipulations using structural models show that the dimer with R = $(CH_2)_3$ has less strain than the dimers with R = $(CH_2)_2$ and $(CH_2)_4$. In the inactive cases, where R = o-C_6H_4, CH_2, $(CH_2)_5$, and $(CH_2)_6$, strains appear to prevent dimerization. Therefore, it is suggested that the 590-nm band is symptomatic of dimerization of $[LMn^{III}H_2O]$ monomers, and complexes that cannot dimerize cannot generate O_2 even if dehydrogenation and deprotonation of the H_2O in the monomer occurs. Oxidized Mn monomers will suffer the same strains preventing dimerization.

H_2O bonded to Mn^{III} in the monomer or as bridges in the Mn^{III} dimer starts off the reaction sequence by transferring a hydrogen atom to an O^- created by a $\pi^* \leftarrow n$ optical excitation in p-benzoquinone. This process oxidizes Mn^{III} to Mn^{IV} and creates tightly bound OH^- groups that are polarized sufficiently for easy deprotonation. It is the formation of the strong Mn–OH bond that prevents the formation of hydroxylated rings, as occurs in aqueous solution in the absence of the active Mn complexes.

The di-μ-oxo Mn^{IV} complex, which forms by either oxidation of the H_2O-bridged Mn^{III} dimer or by dimerization of oxidized monomers, cannot release O_2 because it is too stable. The energetics for a disproportion process where two such dimers come together, and an O_2 molecule forms between them, leaving two $[\{LMn^{III}O\}_2]$, seem feasible and, since all other steps are calculated to be downhill, this is probably the activation step.

The first-order dependence of the reaction rate on the concentration of the initial Mn^{III} complex is consistent with either monomer or dimer participation in the first step. The half-order dependence on p-benzoquinone concentration indicates that there are other reactions occurring.

Acknowledgment. Preparation of this manuscript was assisted by the donors of the Petroleum Research Fund, administered by the American Chemical Society. Md.K.A. is grateful for fellowship support from Tanta University.

Registry No. O_2, 7782-44-7; H_2O, 7732-18-5; $[(H_2N)_2(OH)_2Mn^{III}H_2O]^+$, 117984-04-0; $[\{(H_2N)_2(OH)_2Mn^{III}H_2O\}_2]^{2+}$, 117984-05-1; $[LMn^{III}H_2O]^+$, 104494-13-5; p-benzoquinone, 106-51-4.

Reaction Ergodography for a Model of Siloxane Bond Formation in Organosilane Polymers

Akitomo Tachibana,*,† Hiroyuki Fueno,† Yuzuru Kurosaki,† and Tokio Yamabe†,‡

Contribution from the Department of Hydrocarbon Chemistry, Faculty of Engineering, Kyoto University, Kyoto 606, Japan. *Received May 24, 1988*

Abstract: Reaction ergodography using IRC (intrinsic reaction coordinate) as a unique reaction path is studied for a model of siloxane bond formation in organosilane polymers. This is a dehydrogenation reaction. Using a model system, we have obtained an activation energy of 44.2 kcal/mol and exothermicity of 17.4 kcal/mol (CISD+QC/6-31G**//RHF/3-21G(*)). High reactivity of silicon is found as compared with the reactivity of carbon in an analogue reaction system with the activation energy of 129.2 kcal/mol and the endothermicity of 28.2 kcal/mol (CISD+QC/6-31G**//RHF/3-21G). The present dehydrogenation reaction scheme could be a candidate for a model of siloxane bond formation in organosilane polymers. This is consistent with the mechanism proposed by R. Withnal and L. Andrews (*J. Phys. Chem.* **1985**, *89*, 3261).

I. Introduction

Photolysis of organosilane polymers has received much attention because of their characteristic sensitivity for UV irradiation. Corresponding interests have spread over wide fields of photoresists, photoinitiators for olefin polymerizations or precursors to β-SiC ceramics.[1,2]

The origin for the intense reactivity of organosilane polymers has been shown to be due to the formation of silyl radicals and silylenes as the reaction intermediates. These will produce silylene insertion products and silyl radical derived products.[2] The evidence for the formation of photochemically generated silylene and silyl radicals has been confirmed by West et al. by using alcohol-containing solvents: silylene readily inserts into the oxygen–hydrogen bond, and silyl radicals readily abstract hydrogen radicals and alkoxy radicals from alcohols.[3]

Photolysis of high molecular weight $(PhMeSi)_n$ in degassed THF with excess Et_3SiH, however, leads to complex products such as $Et_3SiO(PhMeSi)H$, $(Et_3Si)_2O$, and $H(PhMeSi)O(PhMeSi)H$. The source of oxygen in these compounds is unknown. The mechanism for the formation of the siloxane bond Si–O–Si[4-7] is

† Also: Division of Molecular Engineering, Graduate School of Engineering, Kyoto University, Kyoto 606, Japan.

‡ Also: Institute for Fundamental Chemistry, 34-4 Takano-Nishihiraki-cho, Sakyo-ku, Kyoto 606, Japan.

(1) See, for example: *Materials for Microlithography: Radiation-Sensitive Polymers*; Thompson, L., Wilson, C. G., Frecht, J. M. J., Eds.; American Chemical Society: Washington, DC, 1984. *Ultrastructure Processing of Ceramics, Glasses and Composites*; Heuch, L., Ulrich, D. R., Eds.; ACS Symposium Series 266; Wiley: New York, 1984.

(2) See, for example: Raabe, G.; Michl, J. *Chem. Rev.* **1985**, *85*, 419.

(3) Trefonas, P., III; West, R.; Miller, R. D. *J. Am. Chem. Soc.* **1985**, *107*, 2737.

(4) (a) Ruelle, P.; Nam-Tran, H.; Buchmann, M.; Kesselring, U. W.; *J. Mol. Struct. THEOCHEM* **1984**, *109*, 177. (b) Chakoumakos, B. C.; Gibbs, G. V. *J. Phys. Chem.* **1986**, *90*, 996. (c) Sauer, J.; Zurawski, B. *Chem. Phys. Lett.* **1979**, *65*, 587. (d) Ernst, C. A.; Allred, A. L.; Ratner, M. A.; Newton, M. D.; Gibbs, G. V.; Moskowitzs, J. W.; Topiol, S. *Chem. Phys. Lett.* **1981**, *81*, 424. (e) Oberhammer, H.; Boggs, J. E. *J. Am. Chem. Soc.* **1980**, *102*, 7241. (f) Grigoras, S.; Lane, T. H. *J. Comput. Chem.* **1987**, *8*, 84.

0002-7863/89/1511-0806$01.50/0 © 1989 American Chemical Society